ANALYSIS OF PRACTICAL SLAB CONFIGURATIONS USING AUTOMATED YIELD-LINE ANALYSIS AND GEOMETRIC OPTIMISATION OF FRACTURE PATTERNS

A.C.A. RAMSAY & D. JOHNSON

Department of Civil & Structural Engineering, The Nottingham Trent University,

Burton Street, Nottingham NG1 4BU, U.K.

[Submitted to the International Journal of Engineering Structures, December 1996]

Keywords: automated yield-line analysis, geometric optimisation, limit analysis and design of slabs.

Abstract: *Automated Yield-Line Analysis* and *Geometric Optimisation* are used in the analysis and design of a number of practical reinforced concrete slab configurations. For two of the chosen configurations comparisons between experimental and theoretical results are possible. The final configuration is included to illustrate the significance and importance of carrying out some form of geometric optimisation.

INTRODUCTION

Whilst it remains important to ensure that elastic deflections remain within acceptable limits, the analysis of reinforced concrete slabs is generally based on plastic rather than elastic considerations. Increasing the load beyond the elastic limit leads to the formation of yield-lines and when sufficient yield-lines have developed so as to form a mechanism, the slab will collapse. The load at which collapse occurs is called the *critical collapse load* and the accurate prediction of this load is important in the limit analysis of slabs.

In the yield-line technique of Johansen[1], a yield-line pattern is postulated for which the corresponding collapse load is then calculated through virtual work. This technique is suitable for determining the critical collapse load for standard configurations of slab where the true collapse mechanism is known *a-priori*. For non-standard configurations, on the other hand, the method needs to be used with caution since, through the upper-bound theorem of plasticity, yield-line patterns which are different from the true one have corresponding collapse loads which are greater than the critical value. The potential for producing unsafe estimates of the critical collapse load can be circumvented, at least to some extent, by comparing solutions for a number of different yield-line patterns. In reference [2] (p664), for example, it is suggested that the investigation of one or two fracture patterns is sufficient to obtain a collapse load that is within 10% of the correct value. However, such 'rules-of-thumb' should be treated with extreme caution for with such limited explorations there is a distinct possibility that either the correct mode will be missed[3,4] or the optimum geometry of the correct mode will not be found[5].

The automated yield-line analysis proposed by Munro & Fonseca[6] provides the basis for a method which can be used to investigate a number of possible fracture patterns simultaneously[7]. The slab is discretised as a mesh of rigid triangular elements with the interelement boundaries and any moment resisting boundary edges being considered as potential yield-lines. In this way the mesh defines a number of potential fracture patterns each having a different collapse load. The pattern with the lowest corresponding

collapse load is the closest to the actual value and the selection is carried out automatically as a linear programming problem.

With a suitable choice of mesh, automated yield-line analysis is generally able to find the correct mode of fracture pattern. However, it is often the case that the geometry of this mode can be optimised and lead to further reductions in the collapse load. The geometric optimisation of fracture pattern has been considered by Jennings et al.[8] and Johnson[9], who choose to use gradient methods (conjugate gradient and sequential linear programming respectively). More recently a direct search strategy (Hooke-Jeeves) has been advocated by Ramsay & Johnson[10]. This strategy has been demonstrated to be convergent and was used to obtain the results presented in this paper. Geometric optimisation is usually carried out after the correct mode of failure has been identified by automated yield-line analysis. A simplified mesh is constructed which includes this mode of failure and the positions of the nodes defining the mode are considered as geometric variables. The optimum positions of the nodes are those which minimise the collapse load.

PRACTICAL EXAMPLES

Whereas references [8,9 & 10] concentrate on theoretical aspects of geometric optimisation and, therefore, only give limited examples, this present paper aims to illustrate the utility of the method through the analysis of a number of practical reinforced concrete slab configurations.

CASE NUMBER 1

This case has been taken from reference [11] in which experimental results are compared with those obtained by the yield-line technique. The correlation between experimental and theoretical results is quite poor and in this present paper automated yield-line analysis and geometric optimisation are applied to see if any improvement can be gained.

A rectangular reinforced concrete slab, simply supported on three edges and free on the fourth has a total load P uniformly distributed over a small central area as shown in Fig. 1. A dead-load of 2.19KN/m^2 is also applied over the entire area of the slab. Isotropic bottom reinforcement is assumed and there is no top reinforcement as indicated in the figure. In this case the purpose of the analysis is to determine the critical collapse load i.e. the magnitude of P that will just cause the slab to collapse.

The yield-line pattern postulated in reference [11] is shown in Fig. 2(a) and the corresponding collapse load is P = 55.4KN. The contours of displacement normal to the plane of the slab corresponding to this yield-line pattern are shown in Fig. 2(b). The amplitude of this mode of displacement is arbitrary and has been chosen such that at the point of maximum displacement, the magnitude is unity. The legend alongside this figure shows the range of displacements corresponding to each gray scale and applies to all subsequent figures in this paper.

The load at which the slab collapsed during the experiment was P = 44KN and the positive and negative yield-line patterns at collapse are shown in Fig. 3(a) and 3(b) respectively.

Whereas in the postulated yield-line pattern the positive yield-line pattern branches from the central yield-line to the corners of the slab, the experimental yield-lines do not reach the corners and terminate on the edge somewhere before the corners. This necessitates the negative fan-type yield-line pattern illustrated in Fig. 3(b). In terms of the collapse load, it is seen that the experimental value is significantly smaller than the theoretical value.

This case is reanalysed using automated yield-line analysis. A symmetric half is analysed and the mesh used is shown in Fig. 4(a). The uniformly loaded region is shown shaded in the figure. As a result of the desirability of using a uniform mesh and the computational limitations on the number of elements used, the width of this region is only modelled approximately (compare the width shown in Fig. 4(a) with that in Fig. 1). The yield-line pattern resulting from the analysis is superimposed onto the mesh, with thick full lines representing positive yield-lines and thick dotted lines representing negative yield-lines. The displacement contours are shown in Fig. 4(b).

The yield-line pattern shown in Fig. 4(a), like that of the experimental slab, indicates the presence of a negative fan-type yield-line. It is interesting to see, however, that unlike both the experimental yield-line pattern and that proposed in reference [11], where the positive yield-line branches at the end of the loaded region, the positive yield-line now branches from within the loaded region. The collapse load, whilst being closer than that obtained by the yield-line technique (Fig. 2), still remains a long way from the experimental value.

In order to improve this solution, geometric optimisation is performed using the simplified mesh shown in Fig. 5(a). The mesh is constructed so as to include the yield-line pattern obtained in the automated yield-line analysis and to allow a more refined representation of the negative fan-type yield-line. The uniformly loaded area is modelled exactly with this mesh.

Six geometric degrees of freedom are considered. These are the x-coordinates of nodes 1,2,3,4 & 5 (see Fig. 5(a) for node numbering) and the y-coordinate of node 2. The optimum solution is shown in Fig. 5(a) and 5(b) and the optimal positions of the nodes are given in Table 1.

Table 1: Nodal coordinates for optimised yield-line pattern of Case 1

Node	x[m]	y[m]
1	0.363	0
2	0.435	0.208
3	0.790	0.550
4	1.139	0.077
5	1.242	0

It is seen that geometric optimisation gives only a small improvement in the solution. The negative fan-type yield-line is modelled more accurately and the positive yield-line pattern is somewhat more complicated than that found previously. The collapse load still over-estimates the experimental value by some 12%. This discrepancy is probably due to difficulties encountered in ensuring uniform bearing and loading conditions for the test and by the conservative criterion used to establish the collapse load from the experimental observations[11].

CASE NUMBER 2

This case has been taken from an investigation carried out by Helba & Kennedy[12] (Bridge Model Number 1) in which results are reported for an experimental investigation, an analysis based on the yield-line technique and for an elastoplastic finite element analysis.

A heavily (45^{o}) skewed bridge deck is simply supported on two edges and is free on the remaining two edges as shown in Fig. 6. A dead-load of 1.3KN/m^2 is applied together with two point loads of equal magnitude P positioned as shown in the figure. These point loads correspond to wheel loads and the problem is to determine their critical value. Orthotropic steel reinforcement is assumed as defined in the figure.

For the automated yield-line analysis reported in this paper a regular mesh is used as shown in Fig. 7(a). The positions of the two point loads do not coincide with any of the nodes in the mesh and statically equivalent nodal forces are therefore applied to the nodes of the elements within which the point loads reside.

The solution achieved by automated yield-line analysis is shown in Fig. 7 and like that of Case 1 a negative fan-type yield-line pattern is obtained. The collapse load corresponding to this yield-line pattern is P = 119.5KN. The fracture pattern of Fig. 7 represents a fan centred around the point loads. A simplified mesh incorporating such a fan-type mechanism is shown in Fig. 8(a). Six geometric degrees of freedom are considered. These are the x- and y-coordinates of nodes 2 & 3 and the positions of nodes 1 & 4 along their respective edges. For this mesh nodes are placed at the precise positions of the point loads. Optimisation of the yield-line pattern results in the pattern shown in Fig. 8(a) and the associated displacement contours given in Fig. 8(b). The collapse load corresponding to this optimised yield-line pattern is P = 101.0KN which represents a 15% reduction in predicted collapse load from that achieved by automated yield-line analysis.

The optimal position of the nodes are given in Table 2.

Table 2: Nodal coordinates for optimised yield-line pattern of Case 2

Node	x[m]	y[m]
1	1.00	1.00
2	1.56	0.89
3	2.38	0.87
4	3.04	0.94

In Table 3, the collapse loads predicted by the automated yield-line analysis and the yield-line pattern optimisation are compared with the values reported in reference [12].

Table 3: Comparison of collapse loads for Case 2

Method	*P*[KN]
automated yield-line analysis	119.5
optimised yield-line pattern	101.0
experimental[12]	105.0
elastoplastic finite element analysis[12]	102.5
yield-line technique[12]	97.5

With the exception of the unoptimised solution predicted by automated yield-line analysis, the collapse loads achieved by the various methods are in close agreement. It will be observed that the manual yield-line analysis of reference [12] produced a lower, and therefore more critical, collapse load than the automated technique employed here. This discrepancy is due to the incorporation of simplifying geometric assumptions in the manual analysis.

CASE NUMBER 3

This case is concerned with the design of a reinforced concrete landing the dimensions of which have been taken from reference [13]. The geometry of the landing is shown in Fig. 9(a) and the mesh to be used in the analysis in Fig. 9(b). A total load of 22.5KN is uniformly distributed over the entire area of the landing. Both top and bottom reinforcements are assumed isotropic and uniform with a moment capacity per unit length of *m* as indicated.

Three different support configurations, as shown in the second column of Fig. 10, are considered whilst the loading is held constant. In configuration 1 the landing is simply supported on two opposite edges. For configuration 2 the back edge of the landing is also simply supported whilst in configuration 3 additional support is offered through a corner column. Configurations 1-3 thus represent increasing levels of support. Results for the three configurations are given in the form of yield-line pattern, displacement contours and moment capacity per unit length respectively in columns 2,3 and 4 of Fig. 10. For configuration 1 the collapse mode is a fairly predictable simple sagging mode. Configuration 2 also has a simple yield-line

pattern with the additional support leading to a reduction of around 85% in the reinforcement requirements.

For configuration 2 the position of the yield-lines is fixed by the corner of the slab and no geometric optimisation is therefore possible. It seems reasonable to assume, therefore, that for this configuration the true mode of failure has been found. For configuration 1, the position of one end of the yield-line is fixed by the corner of the slab. The other end of this yield-line is fixed by the requirement that the yield-lines on the edges of two adjacent parts of the slab pass through the point of intersection of their axes of rotation which, for this case, is at $y = \infty$. Thus, the solution given for configuration 1 is also the true one. For configuration 3, on the other hand, whilst the positions of two of the ends of the yield-lines are fixed by the corners of the slab, the positions of the other ends of the yield-lines can vary and it is possible that geometric optimisation might lead to an increase in reinforcement requirements. Four geometric variables are considered. These are the x-coordinates of nodes 1,2 & 3 (as defined in Fig. 11) and the y-coordinate of node 2.

The optimal positions of the nodes for case 3 are given in Table 4.

Table 4: Nodal coordinates for optimised yield-line pattern of Case 3 (configuration 3)

Node	x[m]	y[m]
1	1.72	1.2
2	2.01	0.51
3	1.86	0

The optimised yield-line pattern and corresponding displacement contours are shown in Fig. 11. This solution was not attainable from the original mesh of Fig. 9(b) since the yield-lines of the optimised solution do not coincide with any of the element edges in the original mesh. The 30% increase in the required reinforcement (which corresponds to a 30% decrease in collapse load for a given level of reinforcement) is very significant indeed and serves to illustrate the importance of including some sort of geometric optimisation in any limit analysis.

It is worth pointing out that the yield-line patterns obtained through automated yield-line analysis are not always easily interpreted and, rather than improving the situation, uniform mesh refinement may actually make interpretation more difficult. Consider, for example, the automated yield-line analysis of the slab used in Case 3 (configuration 3). Fig. 12 shows the results for three uniformly refined meshes.

It is clear that mesh 1 is simply too coarse to provide any reasonable prediction of the failure mode. Mesh 2, which is the same as that used in Case 3, gives a good prediction of the failure mode but does not give the correct geometry of the mode. The results for mesh 3, which embodies both meshes 1 and 2, are interesting. The fact that the results for mesh 3 are different than that for mesh 2 is indicative that the results for mesh 2 are not correct. However, although the results for mesh 3 are clearly closer to the true

solution than those of mesh 2 (c.f. Fig 11), the yield-line pattern is much more complicated and difficult to interpret. The reason for this is that even with a more refined mesh, the available element edges (potential yield-lines) do not coincide with the yield-lines of the optimised geometry. To a certain extent this should not be a cause for concern since the fracture pattern at collapse is of secondary importance to the collapse load or, in this case, the required reinforcement. However, since the results from the automated yield-line analysis are employed in the construction of the simplified meshes used in geometric optimisation, this is a point that should be borne in mind; consider, for example, how one would construct a simplified mesh based on the automated yield-line analysis of mesh 3 alone. Thus, there may be occasions where it is necessary to look at a range of meshes of different degrees of refinement. In the authors' experience, the deflected profile, as indicated by the displacement contours, provides valuable additional information in cases where the yield-line pattern is ambiguous.

A further point, which follows on from the results given in Fig. 12, is that unlike traditional finite element analysis where, in general, it is safe to assume that uniform mesh refinement will lead to convergence to the true solution, in the case of automated yield-line analysis this is not the case. Whilst it is true that uniform mesh refinement will produce monotonically convergent solutions, unless, in the limit as the mesh is refined, the element edges coincide with the yield-lines of the true solution, convergence to the true solution cannot occur.

CONCLUSIONS

Through the examination of the three cases presented, automated yield-line analysis and geometric optimisation have been demonstrated as effective tools for the limit analysis of reinforced concrete slabs. In particular, the crucial requirement of yield-line analysis that the critical collapse mode be established may be satisfied by the initial use of a fine regular mesh of elements. Progressive mesh refinement has been shown not to lead necessarily to an unambiguous prediction of the critical mode. A degree of judgment and experience may therefore be necessary for correct mode elucidation, but deflected profiles can be of considerable assistance in this matter.

Following the establishment of the critical collapse mechanism, a course mesh is used for the purpose of geometric optimisation. The importance of this second phase has been demonstrated by a 30% reduction in collapse load achieved in one instance.

Acknowledgement: The authors are grateful to the reviewers for the constructive criticism offered on this paper.

REFERENCES

1. K.W. Johansen, *Yield Line Theory*, Cement and Concrete Association, London, 1962.

2. A. Ghali and A.M. Neville, *Structural Analysis: A Unified Classical and Matrix Approach*, 3rd edn, E & F.N. Spon, 1996.

3. W.L. Shoemaker, 'Computerized Yield Line Analysis of Rectangular Slabs', *Concrete International*, August, 62-65, (1989).

4. A. Hillerborg, 'Yield Line Analysis', *Concrete International*, May, 9, (1991).

5. D. Johnson, 'Is Yield-Line Analysis Safe?', *proceedings of the Third Canadian Conference on Computing in Civil & Building Engineering*, 494-503, (1996).

6. J. Munro, and A.M.A. da Fonseca, 'Yield Line Method by Finite Elements and Linear Programming', *Structural Engineer*, **56b**(2), 37-44, (1978).

7. K.V. Balasubramanyam and V. Kalyanaraman, 'Yield-Line Analysis by Linear Programming', *J. Struct. Engineering*, **114**(6), (1988).

8. A. Jennings, A. Thavalingam, J.J. McKeown and D. Sloan, *On the Optimisation of Yield Line Patterns*, Developments in Computational Engineering Mechanics, 209-214, B.H.V. Topping, (ed.) Civil-Comp Press, Edinburgh, 1993.

9. D. Johnson, 'Yield-Line Analysis by Sequential Linear Programming', *Int. J. Solids Structures*, **32**(10), 1395-1404, (1994).

10. A.C.A. Ramsay and D. Johnson, 'Geometric Optimisation of Yield-Line Patterns using a Direct Search Method', *accepted for publication in Structural Optimisation*, February (1997).

11. P.A. Wright, *Yield-line Analysis of Reinforced Concrete Slabs*, Final year undergraduate dissertation submitted to the Department of Civil & Structural Engineering of The Nottingham Trent University, 1992.

12. A. Helba and J.B. Kennedy, 'Collapse Loads of Continuous Skew Composite Bridges', Int. J. Struct. Engng., **120**(5), 1395-1413, (1994).

13. P.R. Baker, *Design of L-Shaped Landing Slabs for Carter Concrete Limited*, Final year undergraduate dissertation submitted to the Department of Civil & Structural Engineering of The Nottingham Trent University, 1996.

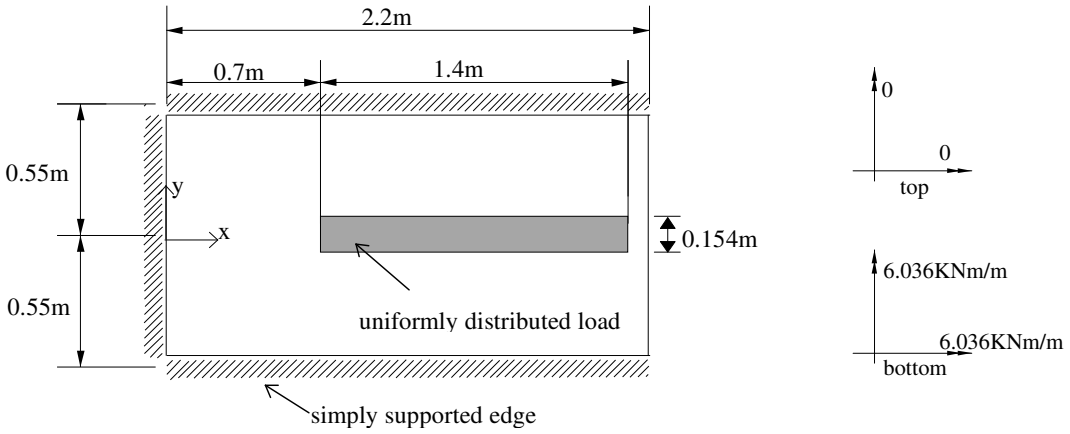

Figure 1: Slab with central strip load (Case 1)

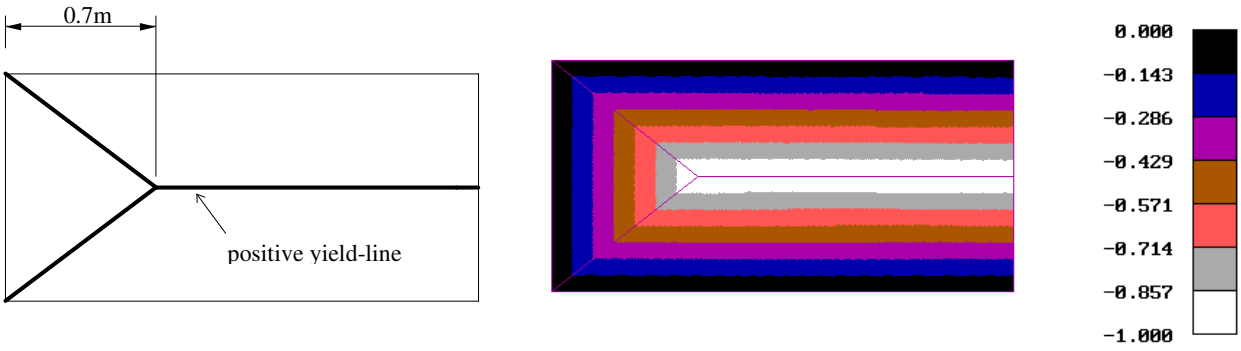

(a) Yield-line pattern (b) Displacement contours (c) Legend

Figure 2: Postulated solution for Case 1 (P = 55.4KN)

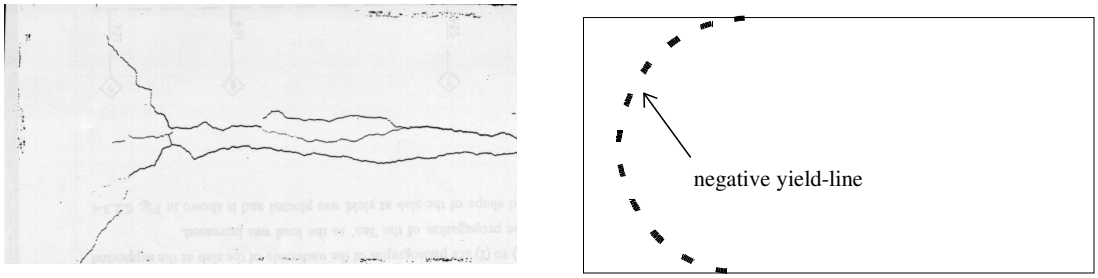

(a) Positive yield-line pattern (photograph) (b) Negative yield-line pattern (schematic)

Figure 3: Experimentally determined yield-line pattern for Case 1 (P = 44KN)

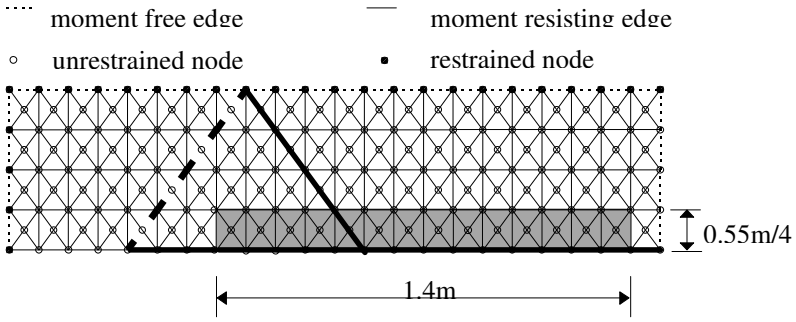

(a) Mesh & yield-line pattern (P = 53.2KN)

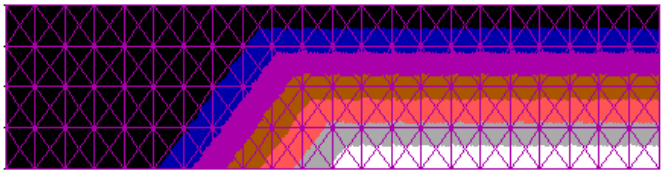

(b) Displacement contours

Figure 4: Results of automated yield-line analysis for Case 1

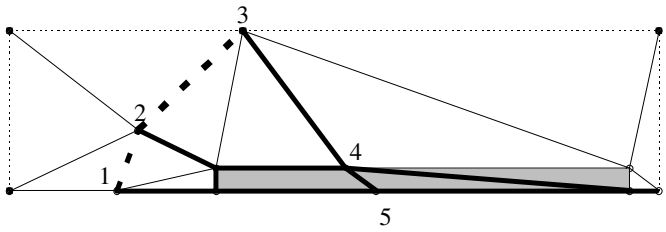

(a) Mesh & yield-line pattern (P = 49.5KN)

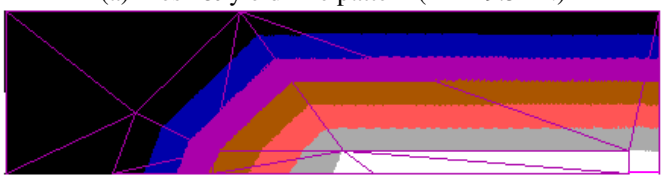

(b) Displacement contours

Figure 5: Optimised yield-line pattern for Case 1

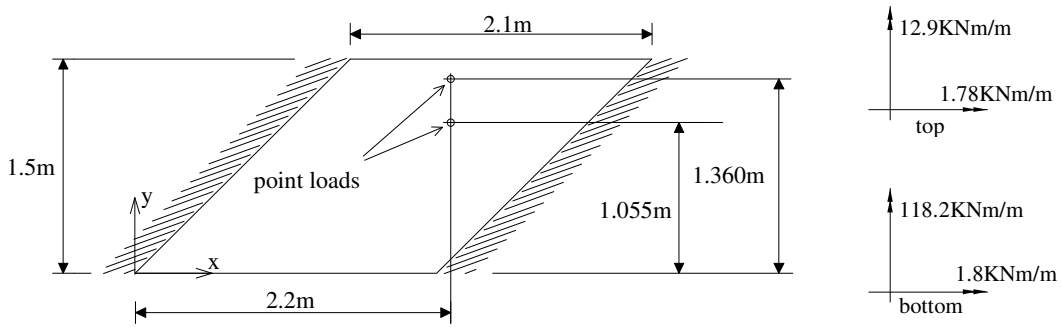

Figure 6: Skewed bridge deck (Case 2)

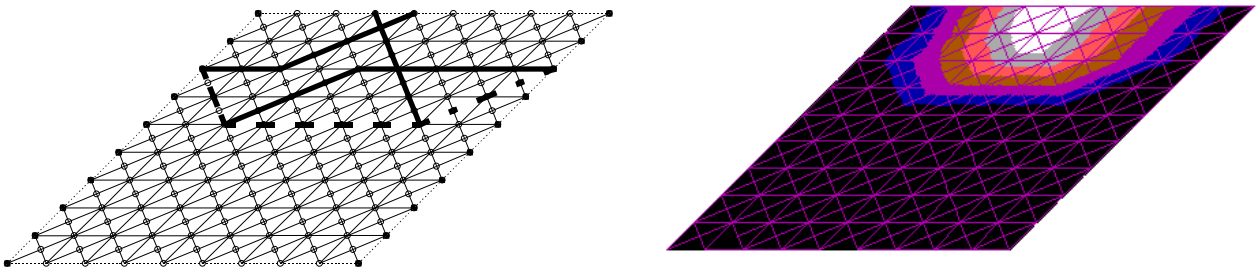

(a) Mesh and yield-line pattern (P = 119.5KN) (b) Displacement contours

Figure 7: Results of automated yield-line analysis for Case 2

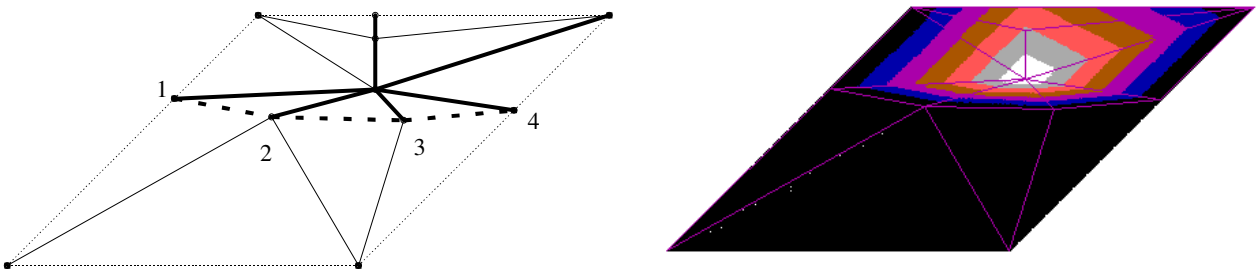

(a) Mesh and yield-line pattern (P = 101.0KN) (b) Displacement contours

Figure 8: Optimised yield-line pattern for Case 2

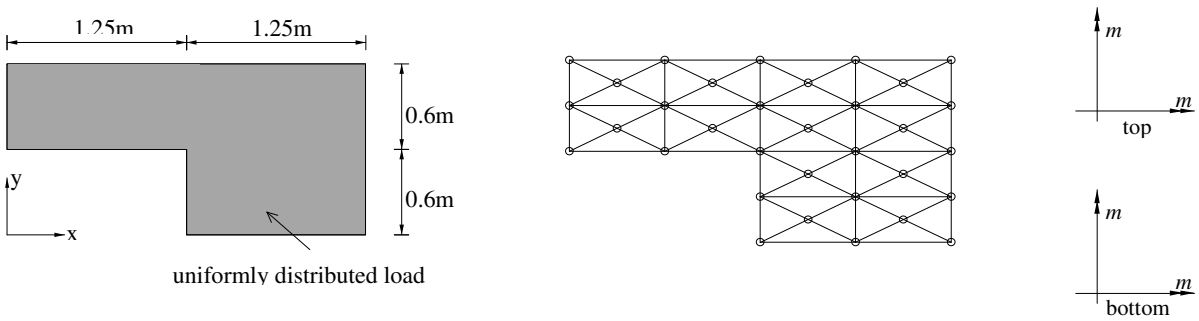

(a) Geometry of landing (b) Mesh

Figure 9: Landing with uniform loading (Case 3)

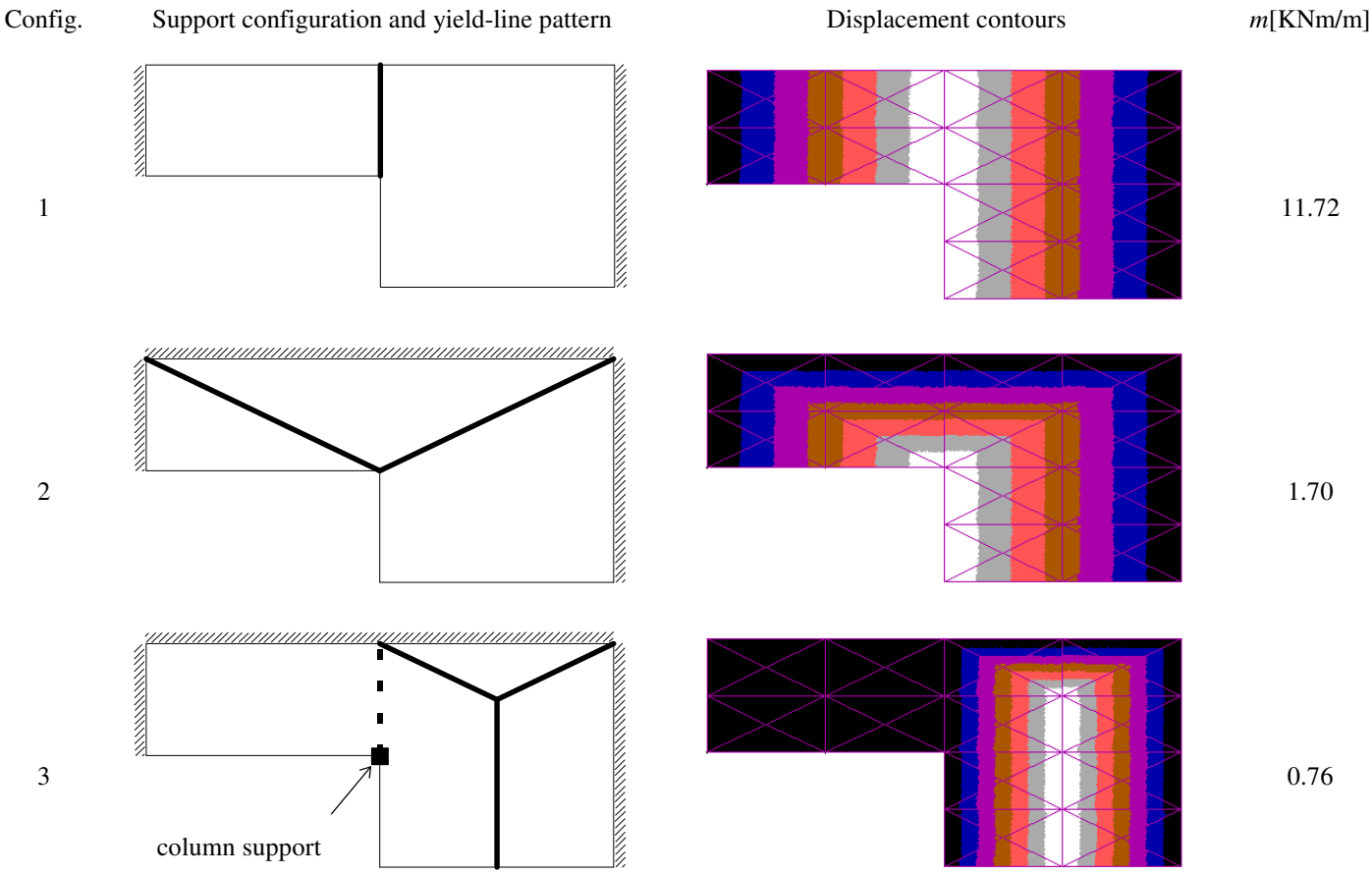

Figure 10: Boundary conditions, yield-line patterns and displacement contours for Case 3

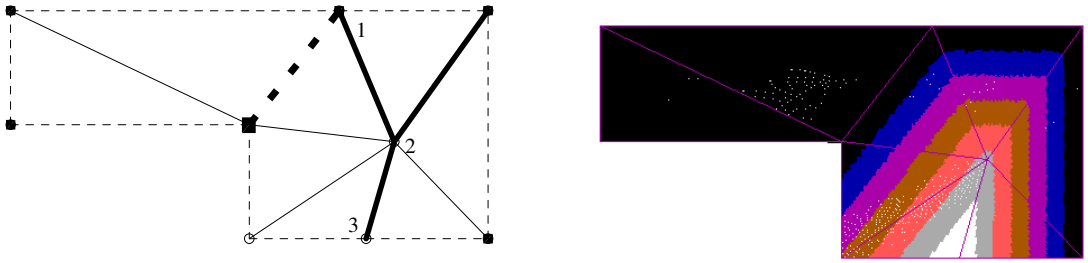

(a) Mesh and yield-line pattern (m = 1.095KNm/m) (b) Displacement contours

Figure 11: Optimised yield-line pattern for Case 3 (configuration 3)

No.	Mesh & yield-line pattern	Displacement contours	*m*[KNm/m]
1	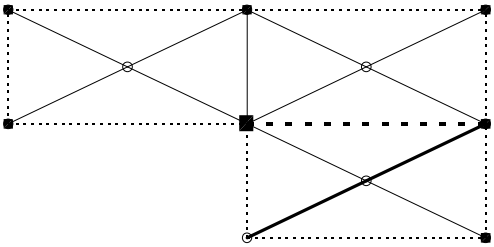	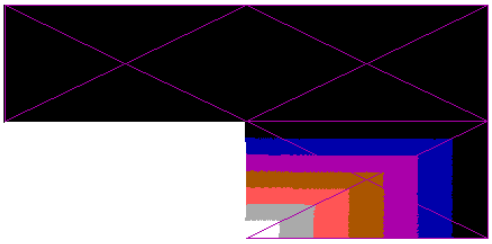	0.538
2	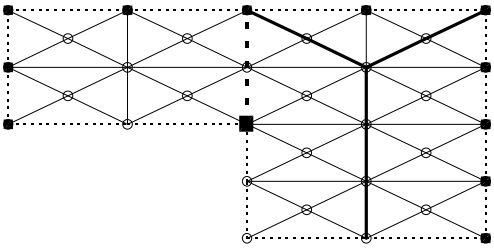	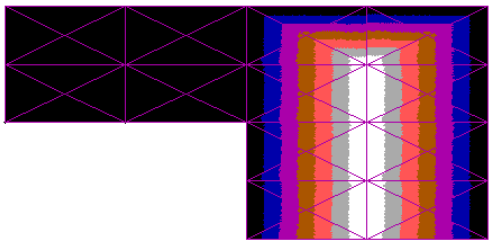	0.766
3	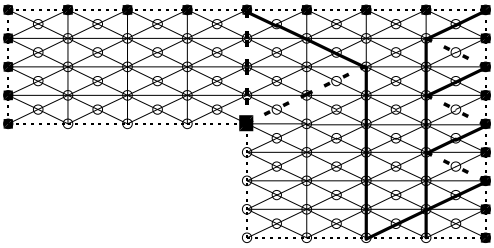	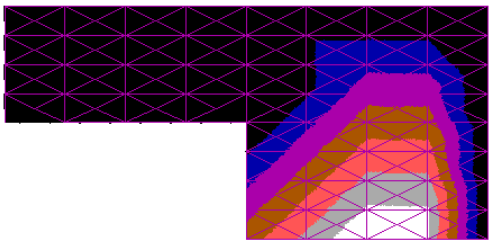	0.777

Figure 12: Convergence of automated yield-line analysis solution for Case 3 (configuration 3)